Journal of Organometallic Chemistry 574 (1999) 66–76

Synthesis, structure and reactivities of novel σ-ruthenocenylplatinum complexes[☆]

Toshiya Yoshida [a], Takahiro Shinohara [a], Kiyotaka Onitsuka [a,*], Fumiyuki Ozawa [a,1], Kenkichi Sonogashira [b,2]

[a] *Department of Applied Chemistry, Faculty of Engineering, Osaka City University, Sumiyoshi-ku, Osaka 558-0022, Japan*
[b] *Department of Applied Science and Chemistry, Faculty of Engineering, Fukui University of Technology, 3-6-1 Gakuen, Fukui 910-8505, Japan*

Received 8 June 1998

Abstract

Novel σ-ruthenocenylplatinum complexes (**3**) and (**4**) have been synthesized by the reaction of trimethylstannylruthenocene (**1**) or 1,1′-bis(trimethylstannyl)ruthenocene (**2**) with Pt(cod)Cl_2, and characterized by means of spectral analyses as well we an X-ray diffraction study. In the cyclic voltammogram of complexes **3** and **4**, irreversible two successive one-electron oxidation peaks of the ruthenocenyl group appear at lower potential than that of irreversible single-step two electron oxidation of ruthenocene. The treatments of σ-ruthenocenylplatinum complex (**5**) with carbon monoxide and aryl isocyanides cause the insertion into Pt–C bond to give insertion products (**7**) and (**9**), respectively. The reaction of **5** with dimethyl or diethyl acetylenedicarboxylate results in the formal insertion of acetylene into the C–H bond of the cyclopentadienyl group at 2-position to give **11** as observed in the reaction of σ-ferrocenyl analog (**6**). Competitive reactions of complexes **5** and **6** with CO, isocyanide or acetylene suggest that the reactivity of **5** towards these substrates is not as high as that of **6**. © 1999 Elsevier Science S.A. All rights reserved.

Keywords: Platinum complex; Ruthenocene; Insertion; Carbon monoxide; Isocyanide; Acetylene

---

1. Introduction

Ferrocene, which is one of the representative organometallic compounds, has been of particular interest ever since its discovery in 1951 because of its unique structure and properties applicable to wide scientific fields [1]. Ruthenocene is a ferrocene analog of ruthenium, and has a typical sandwich structure with larger separation between two cyclopentadienyl rings relative than that of ferrocene [2,3]. In contrast to a reversible one electron redox behavior of ferrocene, ruthenocene shows an irreversible one-step two electron oxidation at a higher potential than that of ferrocene [4].

Recently metallocenyl transition-metal complexes have been received much attention since some of which show an intramolecular interaction between transition-metal atom and a central metal atom of metallocenyl ligand [5]. In the course of our study on σ-ferrocenylplatinum complexes, we have found that a ferrocenyl group acts as an electron pool controlling the reactivity of a platinum center [6]. Thus, σ-ferrocenylplatinum complexes show characteristic reactivities with CO, isocyanide and acetylene [7,8]. The remarkable feature of ruthenocene has led us to the chemistry of σ-ruthenocenylplatinum complexes, which may show the different or specific reactivity with relative to that of σ-ferrocenyl analog owing to the electronic and/or structural feature of the ruthenocenyl ligand. In comparison with many publications on σ-fer-

---

[☆] Dedicated to the late Professor Rokuro Okawara on the occasion of his memorial issue.

[*] Corresponding author. Present address: Institute of Scientific and Industrial Research, Osaka University, Ibaraki, Osaka 567-0047, Japan.

[1] Also corresponding author.

[2] Also corresponding author.

0022-328X/99/$ - see front matter
PII: S0022-328X(98)00972-3

rocenyl transition-metal complexes, a limited number of studies on σ-ruthenocenyl transition-metal complexes have appeared in the literature [9]. Thus, we present here the synthesis of novel σ-ruthenocenylplatinum complexes and their reactivity of Pt–C bond toward insertion of CO, isocyanide and acetylene.

2. Results and discussion

2.1. Syntheses of σ-ruthenocenylplatinum complexes

As a synthetic strategy of σ-ruthenocenylplatinum complexes, transmetallation of trimethylstannylruthenocene with Pt(cod)Cl$_2$, that is a similar method used for the synthesis of σ-ferrocenylplatinum complex [10], was chosen. Treatment of ruthenocene with excess *n*-BuLi (ca. 2.4 equivalents) in THF at −50°C followed by treatment with trimethylstannylchloride at 0°C gave a mixture of ruthenocene, trimethylstannylruthenocene (**1**) and 1,1′-bis(trimethylstannyl)ruthenocene (**2**) in a 1:6:3 molar ratio (determined by GLC analysis). Since we could not isolate complexes **1** and **2**, this mixture was treated with Pt(cod)Cl$_2$ in refluxing THF and the resulting products were separated by column chromatography on alumina. RcPt(cod)Cl (Rc = (C$_5$H$_4$)Ru(C$_5$H$_5$)) (**3**) and {C$_5$H$_4$Pt(cod)Cl}$_2$Ru (**4**) were obtained from benzene fraction in 64% yield and from CH$_2$Cl$_2$ fraction in 37% yield, respectively. These complexes **3** and **4** are air and moisture stable at ambient temperature both in the solid state and in solution. Characterization of these complexes was made by the ^{1}H- and ^{13}C-NMR spectra as well as an X-ray analysis (Scheme 1).

The ^{1}H-NMR spectrum of **3** showed two triplet signals at δ 5.60 and 5.11 attendant with ^{195}Pt satellite peaks ($^2J_{\mathrm{Pt-H}} = 29.3$ and 74.7 Hz, respectively) attributed to olefinic protons of a cod ligand, along with two triplets of substituted cyclopentadienyl protons at δ 4.69 and 4.60, and a singlet of non-substituted cyclopentadienyl protons at δ 4.59. The resonances of cyclopentadienyl protons of **3** appeared much lower field than those of σ-ferrocenyl analogs, FcPt(cod)Cl (Fc = (C$_5$H$_4$)Fe(C$_5$H$_5$)) [11], suggesting the lower electron density of the cyclopentadienyl rings in the ruthenocenyl compounds relative to ferrocenyl analogs [12]. Similar shifts of the signals attributed to substituted cyclopentadienyl protons into lower magnetic field was also observed in the ^{1}H-NMR spectrum of **4**.

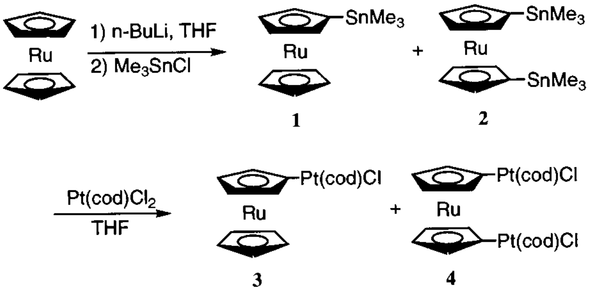

Scheme 1.

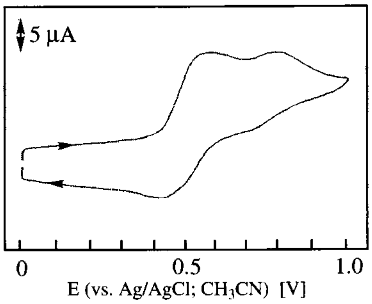

Fig. 1. Cyclic voltammogram of **3** (1.9 × 10^{-3} M in CH$_2$Cl$_2$); scan rate 100 mV s^{-1}, supporting electrolyte Bu$_4$NPF$_6$ (1.0 × 10^{-1} M), working electrode Pt-disk (2 mm diameter).

Subsequently, the electrochemical properties of **3** and **4** were studied by cyclic voltammetry. In contrast to a reversible one-electron redox behavior of the ferrocenyl group in FcPt(cod)Cl [11], the cyclic voltammogram of **3** (Fig. 1) exhibited irreversible two successive one-electron oxidation peaks of the ruthenocenyl moiety $E_a =$ 0.53 V (Ru$^{\mathrm{II}}$/Ru$^{\mathrm{III}}$); 0.80 V (Ru$^{\mathrm{III}}$/Ru$^{\mathrm{IV}}$) relative to Ag/AgCl at the Pt-disc electrode in dichloromethane solution. If one considers that ruthenocene undergoes an irreversible single-step two electron oxidation at $E_a = 0.88$ V, it appears that the platinum fragment strongly donates electron density to the ruthenocenyl group and stabilizes the ruthenocenium cation fragment [11,13]. Complex **4** also showed similar oxidation behavior at lower potential $E_a = 0.35$ V (Ru$^{\mathrm{II}}$/Ru$^{\mathrm{III}}$); 0.58 V (Ru$^{\mathrm{III}}$/Ru$^{\mathrm{IV}}$) relative to Ag/AgCl in the cyclic voltammogram as shown in Fig. 2. The shift of oxidation potential of **4** relative to **3** is also explained by the strong electron donation of the platinum moieties.

The molecular structure of **3** is shown in Fig. 3 and selected bond lengths and angles are given in Table 1. The environment of the Pt atom is the expected square-planar with σ-bond to the ruthenocenyl group and

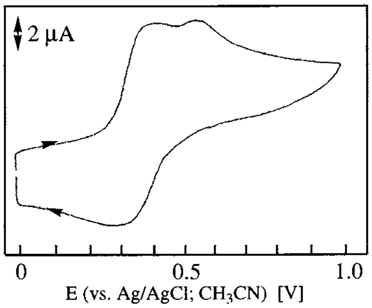

Fig. 2. Cyclic voltammogram of **4** (1.0 × 10^{-3} M in CH$_2$Cl$_2$); scan rate 100 mV s^{-1}, supporting electrolyte Bu$_4$NPF$_6$ (1.0 × 10^{-1} M), working electrode Pt-disk (2 mm diameter).

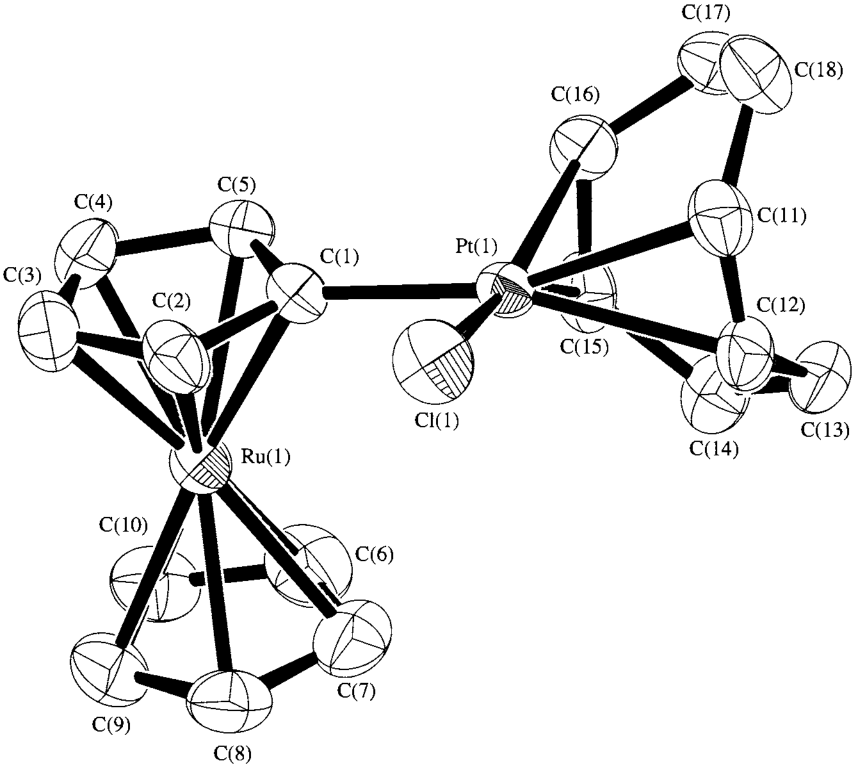

Fig. 3. Molecular structure of **3**. Hydrogen atoms have been omitted for clarity.

π-bonds to the cyclooctadiene ligand. The Pt(1)–C(1) bond length *trans* to cyclooctadiene is 2.033(5) Å, which is comparable to those observed in Pt(cod)$\{Fe(C_5H_4Cl)(C_5H_3Cl)\}_2$ (2.003(19) and 2.042(16) Å) [14] and $\{C_5H_4Pt(cod)Cl\}Mn(CO)_3$ (2.04(1) Å) [15]. The Pt(1)–C(11) and Pt(1)–C(12) bond lengths (2.284(6) and 2.315(5) Å) are longer than those of Pt(1)–C(15) and Pt(1)–C(16) (2.126(6) and 2.155(5) Å), and the bond distance of C(11)–C(12) (1.367(8) Å) is shorter than that of C(15)–C(16) (1.392(8) Å). These phenomena are due to the difference of *trans* influence between the ruthenocenyl group and the Cl ligand. The dihedral angle between the plane containing Pt(1), C(1) and Cl(1), and the cyclopentadienyl ring consisting of C(1)–C(5) is 14.6°. The two cyclopentadienyl rings are essentially parallel and the ruthenocenyl group has an eclipsed conformation.

Table 1
Selected bond lengths (Å) and angles (°) for **3**

Bond lengths (Å)			
Pt(1)–C(1)	2.033(5)	Pt(1)–C(16)	2.155(5)
Pt(1)–C(11)	2.284(6)	Pt(1)–Cl(1)	2.319(2)
Pt(1)–C(12)	2.315(5)	C(11)–C(12)	1.367(8)
Pt(1)–C(15)	2.126(6)	C(15)–C(16)	1.392(8)
Bond angles (°)			
Cl(1)–Pt(1)–C(1)	91.2(2)	C(11)–Pt(1)–C(16)	95.7(2)
Cl(1)–Pt(1)–C(11)	86.9(2)	C(11)–Pt(1)–C(12)	34.6(2)
Cl(1)–Pt(1)–C(12)	92.4(2)	C(12)–Pt(1)–C(15)	80.4(2)
C(1)–Pt(1)–C(15)	91.3(2)	C(15)–Pt(1)–C(16)	37.9(2)
C(1)–Pt(1)–C(16)	95.0(2)		

The molecular structure of **4** is also illustrated in Fig. 4 and selected bond lengths and angles are listed in Table 2. As expected from ^1H- and ^{13}C-NMR spectra, two platinum atoms are σ-bonded to both cyclopentadienyl rings and the coordination around the each platinum atom is similar to that of **3**. It may be of interest that two bulky platinum moieties are closely located each other by the rotation of cyclopentadienyl groups. However, the distance between Pt(1) and Pt(2) is 4.5983(9) Å, suggesting no direct interaction between two platinum atoms. The distances of Pt(1)–Cl(2) and Pt(2)–Cl(1) are > 4 Å, which are clearly in the range of nonbonding distances. Therefore, the conformation of cyclopentadienyl groups bound to a platinum moiety is likely due to crystal-packing force.

Complex **3** was easily converted to a phosphine analog **5** by a ligand-exchange reaction. Thus, treatment of **3** with triethylphosphine gave complex **5a** in 85% yield. Treatment of **5a** with excess NaBr or NaSCN in methanol caused an exchange of an anion ligand to give **5b** and **5c**, respectively. Since slow evaporation of hexane solution of **5c** gave fine crystals, an X-ray analysis was performed. There are two independent molecules with essentially the same structure in a unit cell. One of the two molecular structures of **5c** is shown in Fig. 5 and selected bond lengths and angles are listed in Table 3. Pt–C bond lengths are 2.032(8)

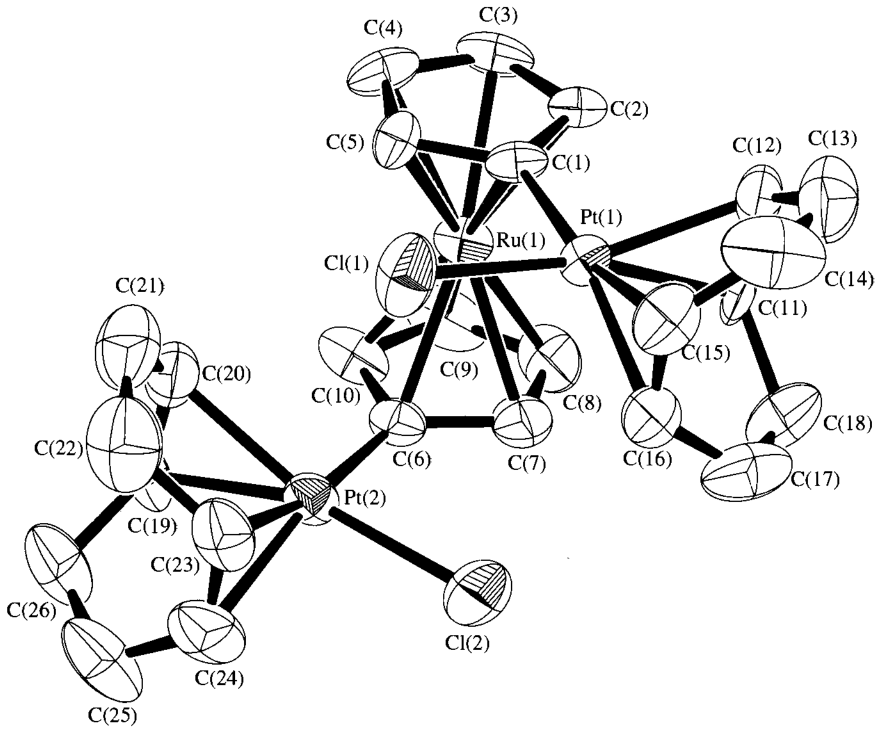

Fig. 4. Molecular structure of **4**. Hydrogen atoms have been omitted for clarity.

and 2.030(8) Å, respectively. These values are comparable those of σ-ruthenocenylplatinum complexes (vide supra). Since a bulky platinum group is directly linked to the cyclopentadienyl group, the ruthenocenyl moiety has a strained structure with the tilt angle between two cyclopentadienyl planes of 10.1 and 9.3°, respectively [8]. The platinum atoms lie at a distance of 0.61 or 0.63 Å from the plane of the bound cyclopentadienyl group, which is also due to the steric effect of the bulky platinum moiety. The coordination planes around Pt atoms make dihedral angles with the cyclopentadienyl planes of 80.3 and 81.7°, respectively.

Table 2
Selected bond lengths (Å) and angles (°) for **4**

Bond lengths (Å)			
Pt(1)–C(1)	2.031(9)	Pt(2)–C(6)	2.030(9)
Pt(1)–C(11)	2.13(1)	Pt(2)–C(19)	2.12(1)
Pt(1)–C(12)	2.16(1)	Pt(2)–C(20)	2.14(1)
Pt(1)–C(15)	2.27(1)	Pt(2)–C(23)	2.26(1)
Pt(1)–C(16)	2.28(1)	Pt(2)–C(24)	2.27(1)
Pt(1)–Cl(1)	2.342(3)	Pt(2)–Cl(2)	2.317(3)
C(11)–C(12)	1.38(1)	C(19)–C(20)	1.39(2)
C(15)–C(16)	1.36(2)	C(23)–C(24)	1.37(2)
Bond angles (°)			
Cl(1)–Pt(1)–C(1)	91.1(3)	Cl(2)–Pt(2)–C(6)	91.9(3)
Cl(1)–Pt(1)–C(15)	87.7(4)	Cl(2)–Pt(2)–C(23)	90.4(4)
Cl(1)–Pt(1)–C(16)	92.4(2)	Cl(2)–Pt(2)–C(24)	88.2(4)
C(1)–Pt(1)–C(11)	92.6(4)	C(6)–Pt(2)–C(19)	93.1(4)
C(1)–Pt(1)–C(12)	93.4(4)	C(6)–Pt(2)–C(20)	91.3(4)
C(11)–Pt(1)–C(16)	81.2(4)	C(19)–Pt(2)–C(24)	80.9(5)
C(15)–Pt(1)–C(16)	34.8(4)	C(19)–Pt(2)–C(20)	38.0(5)
C(12)–Pt(1)–C(15)	81.7(5)	C(20)–Pt(2)–C(23)	81.6(5)
C(11)–Pt(1)–C(12)	37.7(4)	C(23)–Pt(2)–C(24)	35.1(5)

2.2. Reaction of carbon monoxide, aryl isocyanide and acetylene with σ-ruthenocenylplatinum complexes

In analogy with σ-ferrocenylplatinum complexes (**6**), reactions of σ-ruthenocenylplatinum complexes **5** with CO, aryl isocyanide and acetylene having an electron-withdrawing group were investigated (Scheme 2). When complex **5a** was treated with 30 kg cm^{-2} of CO at room temperature (r.t.) for 24 h pale yellow crystals of *trans*-RcC(O)Pt(PEt$_3$)$_2$Cl (**7a**) were obtained in 88% yield. The IR and ^{13}C-NMR spectra indicated that **7a** was produced by insertion of CO into the Pt–C bond of **5a**. The CO stretching vibration was observed at 1610 cm^{-1} in the IR spectrum of **7a**. The resonance attributed to carbonyl carbon appeared at δ 211.6 in the ^{13}C-NMR spectrum [7]. It is noteworthy that the insertion of CO into the Pt–C bond occurs at r.t. as observed σ-ferrocenyl platinum analogs **6** though the carbonylation of *trans*-RPt(PR$'_3$)$_2$X was achieved at 90°C [16]. The similar treatment of **5b** gave the insertion product, *trans*-RcC(O)Pt(PEt$_3$)$_2$Br (**7b**), in 88% yield, but the reaction of **5c** with CO afforded the acylplatinum complex **7c** in only 11% yield.

On treatment of **5a** with 1.2 equivalent of p-tolylisocyanide in refluxing 1,2-dichloroethane for 6 h, a yellow complex, *trans*-RcC(=NC$_6$H$_4$Me-p)Pt(PEt$_3$)$_2$Cl (**9a**), which is resulted from insertion of isocyanide into the

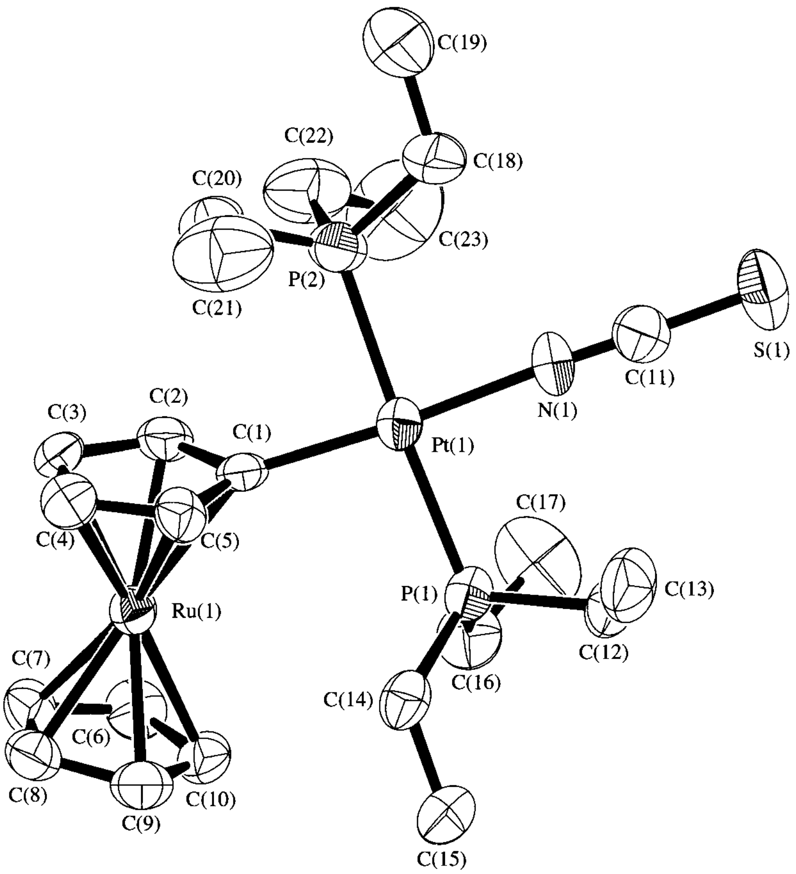

Fig. 5. Molecular structure of **5c**. Hydrogen atoms have been omitted for clarity.

Pt–C bond of **5a**, was isolated in 63% yield. The insertion of isocyanide is revealed by the ν(C=N) absorption at 1550 cm^{-1} in the IR spectrum of **9a** and the resonance of iminoacyl carbon at δ 172.1 in the ^{13}C-NMR spectrum [7]. ^{31}P-NMR spectrum of **9a** showed a singlet signal at δ 14.70 with satellite signals due to the coupling of ^{195}Pt nucleus ($J_{\text{Pt–P}} = 2894$ Hz), indicating the *trans* conformation around the Pt atom. ^{1}H-NMR spectrum and the results of elemental analysis were also consistent with the structure of **9a**. The reaction of **5a** with 2,6-xylyl or *p*-nitrophenyl isocyanide in a similar manner also afforded the insertion product, *trans*-RcC(=NC$_6$H$_3$Me$_2$-2,6)Pt(PEt$_3$)$_2$Cl (**9b**) or *trans*-RcC(=NC$_6$H$_4$NO$_2$-*p*)Pt(PEt$_3$)$_2$Cl (**9c**), in 36 and 50% yields, respectively.

The molecular structure of **9a** is shown in Fig. 6. *p*-Tolyl isocyanide is undoubtedly inserted into the Pt–C bond of **5a** to form iminoacylplatinum complex and the coordination sphere around the Pt atom is a

Table 3
Selected bond lengths (Å) and angles (°) for **5c**

Bond lengths (Å)			
Pt(1)–P(1)	2.293(3)	Pt(2)–P(3)	2.296(2)
Pt(1)–P(2)	2.329(3)	Pt(2)–P(4)	2.317(3)
Pt(1)–N(1)	2.039(7)	Pt(2)–N(2)	2.070(8)
Pt(1)–C(1)	2.032(8)	Pt(2)–C(31)	2.030(8)
Bond angles (°)			
P(1)–Pt(1)–P(2)	176.17(9)	P(3)–Pt(2)–P(4)	175.36(9)
P(1)–Pt(1)–N(1)	89.3(2)	P(3)–Pt(2)–N(2)	89.2(2)
P(1)–Pt(1)–C(1)	94.9(2)	P(3)–Pt(2)–C(31)	94.6(2)
P(2)–Pt(1)–N(1)	87.9(2)	P(4)–Pt(2)–N(1)	87.9(2)
P(2)–Pt(1)–C(1)	87.8(2)	P(4)–Pt(2)–C(31)	88.2(2)
N(1)–Pt(1)–C(1)	175.7(3)	N(2)–Pt(2)–C(31)	175.8(3)

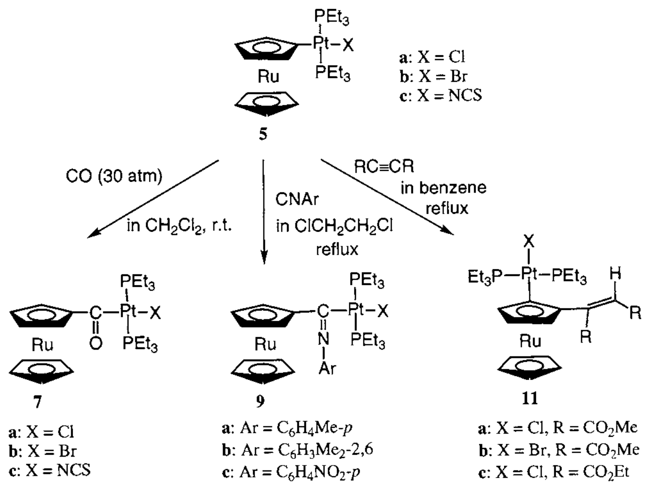

Scheme 2.

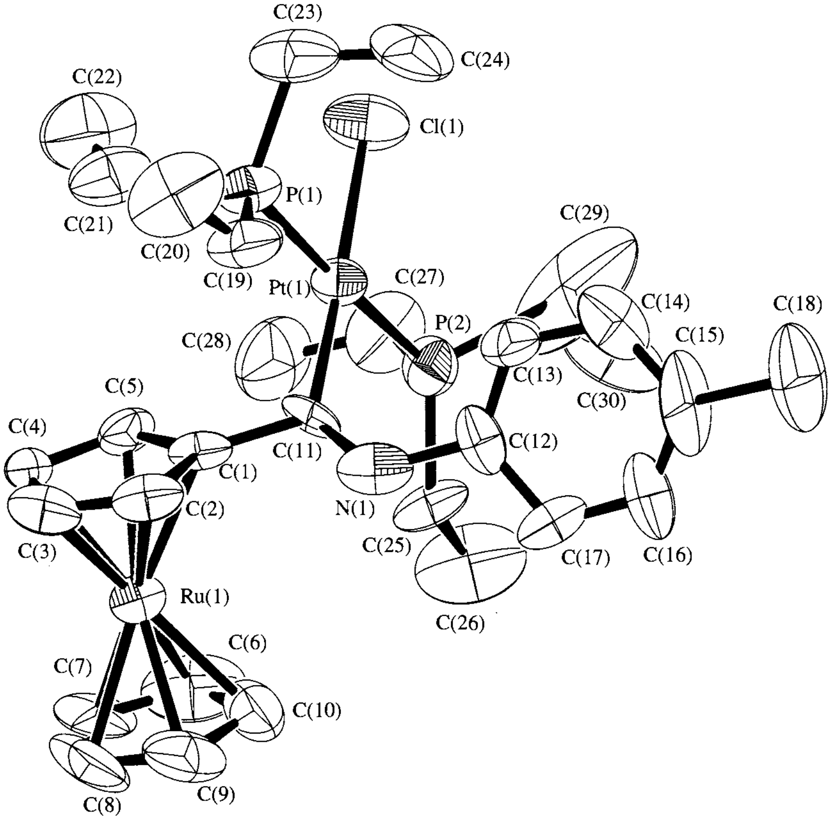

Fig. 6. Molecular structure of **9a** · CHCl$_3$. Hydrogen atoms and a solvent molecule have been omitted for clarity.

square-planar with two PEt$_3$ ligands in mutually *trans* positions. Table 4 lists selected bond lengths and angles. The Pt(1)–C(11) bond length of 2.03(2) Å is comparable with those of other *trans*-iminoacylplatinum complexes [17]. The Pt(1)–Cl(1) bond distance is 2.438(5) Å, which is longer than those of **3** and **4** (vide supra) and comparable to that of *trans*-FcC(O)Pt(PEt$_3$)$_2$Cl (**8**) (2.441(2) Å) [7], indicating the strong *trans* influence of the iminoacyl group as well as an acyl group. The plane of the iminoacyl group defined by Pt(1), C(11), C(1), N(1) and C(12) makes dihedral angles with the Pt coordination plane and the cyclopentadienyl ring C(1)–C(5) for 72.8 and 31.1°, respectively. The former is smaller than that of a ferrocenyl analog (**10**) having a *cis* geometry, while the latter is larger than that of **10** [7]. The tilt angle between two cyclopentadienyl rings of the moiety ruthenocene is 0.8°.

Table 4
Selected bond lengths (Å) and angles (°) for **9a** · CHCl$_3$

Bond lengths (Å)			
Pt(1)–Cl(1)	2.438(5)	C(1)–C(11)	1.50(3)
Pt(1)–P(1)	2.320(6)	N(1)–C(11)	1.230(2)
Pt(1)–P(2)	2.299(6)	N(1)–C(12)	1.43(2)
Pt(1)–C(11)	2.03(2)		
Bond angles (°)			
Cl(1)–Pt(1)–P(1)	90.1(2)	P(2)–Pt(1)–C(11)	92.4(6)
Cl(1)–Pt(1)–P(2)	87.3(2)	Pt(1)–C(11)–C(1)	115(1)
Cl(1)–Pt(1)–C(11)	177.7(6)	Pt(1)–C(11)–N(1)	127(2)
P(1)–Pt(1)–P(2)	177.3(2)	N(1)–C(11)–C(1)	117(1)
P(1)–Pt(1)–C(11)	90.2(6)	C(11)–N(1)–C(12)	124(2)

Complex **5a** was treated with slight excess of dimethylacetylenedicarboxylate (DMAD) in benzene at reflux temperature for 24 h and the yellow crystals of **11a** was obtained in 25% yield. The IR spectrum of **11a** showed a ν(C=C) absorption at 1610 cm^{-1} and two ν(C=O) absorptions at 1735 and 1705 cm^{-1}. The ^{1}H-NMR spectrum exhibited a signal of the olefinic proton at δ 7.94 and three resonances of the substituted cyclopentadienyl ring protons at δ 4.67, 4.63 and 4.52. All of the spectroscopic data (IR, ^{1}H-, ^{13}C- and ^{31}P-NMR) for **11a** are similar to those of a ferrocenyl analog (**12a**) (X = Cl; R = CO$_2$Me) [8], indicating that **11a** has a similar structure to that of **12a**, i.e. **11a** was produced by the formal insertion of DMAD into the C–H bond at 2-position of the ruthenocenyl group. Similar treatments of **5b** with DMAD and **5a** with diethyl acetylenedicarboxylate afforded **11b** in 40% yield and **11c** in 30% yield, respectively. The reaction mechanism of the formation of **11** will be identical with that of **12** as previously reported.

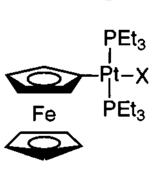

6

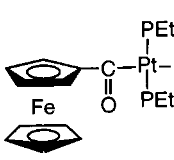

8

Table 5
Crystallographic data for **3**, **4**, **5c** and **9a**·$CHCl_3$

	3	**4**	**5c**	**9a**·$CHCl_3$
Formula	$C_{18}H_{21}ClPtRu$	$C_{26}H_{32}Cl_2Pt_2Ru$	$C_{23}H_{39}NP_2PtRuS$	$C_{31}H_{47}Cl_4NP_2PtRu$
M_W	568.98	906.69	719.74	933.64
Color, habit	Yellow, prismatic	Colorless, needle	Pale yellow, plate	Yellow, prismatic
Crystal size (mm)	0.35 × 0.25 × 0.25	0.25 × 0.07 × 0.02	0.25 × 0.25 × 0.10	0.30 × 0.20 × 0.10
Crystal system	Monoclinic	Monoclinic	Triclinic	Monoclinic
Lattice parameters	$a = 10.719(2)$ Å $b = 10.834(2)$ Å $c = 14.342(2)$ Å $\beta = 102.47(1)°$ $V = 1626.3(3)$ Å^3	$a = 12.515(2)$ Å $b = 10.170(2)$ Å $c = 18.961(2)$ Å $\beta = 93.70(1)°$ $V = 2408.2(6)$ Å^3	$a = 17.236(3)$ Å $b = 20.631(5)$ Å $c = 7.734(2)$ Å $\alpha = 99.63(2)°$ $\beta = 94.58(2)°$ $\gamma = 86.18(2)°$ $V = 2705(1)$ Å^3	$a = 16.548(4)$ Å $b = 13.128(3)$ Å $c = 17.010(4)$ Å $\beta = 96.62(2)°$ $V = 3670(1)$ Å^3
Space group	$P2_1/n$ (no. 14)	$P2_1/c$ (no. 14)	$P\bar{1}$(no. 2)	$P2_1/n$ (no. 14)
Z	4	4	4	4
$D_{calc.}$ (g cm^{-3})	2.324	2.501	1.767	1.689
μ(Mo–K$_{\alpha\alpha}$) (cm^{-1})	97.52	125.58	59.70	46.52
2θ range (°)	$6<2\theta<55.1$	$6<2\theta<50.1$	$6<2\theta<50.1$	$6<2\theta<50.2$
No. of reflections measured	3956	4531	9920	7065
No. of observed reflections	2979 ($I>3.0\sigma(I)$)	3136 ($I>3.0\sigma(I)$)	6718 ($I>3.0\sigma(I)$)	2807 ($I>2.0\sigma(I)$)
No. of variables	190	280	523	361
Residuals: R; R_w	0.026; 0.029	0.032; 0.036	0.036; 0.035	0.064; 0.056
Goodness-of-fit	1.59	1.38	1.39	1.25
Max; min (Δ/ρ) (e Å^{-3})	0.95; −2.32	1.09; −0.92	1.49; −1.29	0.87; −1.47

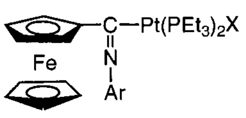

10

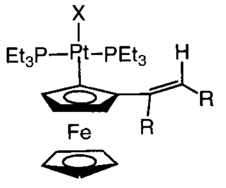

12

As shown above, reaction of σ-ruthenocenylplatinum complexes **5** with CO, aryl isocyanide and acetylene having an electron-withdrawing group under the same conditions for σ-ferrocenylplatinum analog **6** gave similar insertion products **7**, **9** and **11**, respectively. Consequently, reactivity of σ-ruthenocenylplatinum complex **5** toward insertion reactions was compared with those of σ-ferrocenylplatinum analog **6**. A competitive reaction of complexes **5a** and **6a** (X = Cl) with atmospheric pressure of CO at r.t. (about 20°C) in benzene giving acylplatinum complexes, **7a** and **8a** (X = Cl), was monitored by ^{31}P-NMR spectroscopy. The carbonylation of **6a** is ca. 11 times faster than that of **5a**. Similarly, the insertion of p-nitrophenyl isocyanide into the Pt–C bond of **6a** is about 300 times faster than that of **5a** at r.t. in 1,2-dichloroethane. The rate of the reaction of **6a** with DMAD was also is ca. 2.5 times faster than that of **5a**. These results indicate that reactivity of σ-ruthenocenylplatinum complex **5a** toward CO, isocyanide and acetylene insertions is lower than that of σ-ferrocenylplatinum analog **6**. A study on the mechanism of CO insertion into a Pt–C bond has shown that an electron-donating substituent of an organic group enhances the rate of CO insertion [18]. Although metallocenyl groups are a strong electron-donating group, electron density of the cyclopentadienyl ring of ferrocene is higher than that of ruthenocene as suggested by the ^{1}H-NMR spectra of **5a** and **6a** (vide supra) [12]. Therefore, the lower electron-donating feature of a ruthenocenyl group than that of a ferrocenyl group may causes the difference in the reactivity between σ-ruthenocenyl- and σ-ferrocenylplatinum complexes. The result that the carbonylation of $\{C_5H_4Pt(cod)Cl\}Mn(CO)_3$ requires heating at 100°C is consistent with this explanation [15].

3. Experimental

All reactions except for the reaction with carbon monoxide were performed under a nitrogen atmosphere, and the workup was carried out in air. ^{1}H-, ^{13}C- and ^{31}P-NMR spectra were measured on a JEOL α400 spectrometer. For ^{1}H and ^{13}C-NMR $SiMe_4$ was used as an internal standard, and ^{31}P-NMR spectra were referred to an external standard of PPh_3. IR spectra were recorded on a JASCO A-202 spectrometer. Cyclic voltammetric measurement was performed in CH_2Cl_2 at r.t. with 0.1 M tetrabutylammonium hexafluorophosphate as supporting electrolyte and the scan rate was 100 mV s^{-1}. The reference electrode was Ag/AgCl (acetonitrile) and working electrode was a platinum-disc electrode (2 mm diameter). All chemicals were used as received and aryl isocyanide were prepared according to the literature method [19].

*3.1. Preparation of trimethylstannylruthenocene (**1**) and 1,1′-bis(trimethystannyl)ruthenocene (**2**)*

A 1.6 M solution of *n*-BuLi in hexane (10.0 ml, 16.0 mmol) was added dropwise to a solution of ruthenocene (1.516 g, 6.555 mmol) in THF (50 ml) at −50°C. After stirring for 1 h at −50°C, the reaction mixture was allowed to warm slowly to r.t. and stirred for an additional 20 h. Then to a reaction mixture was added dropwise a solution of Me_3SnCl (2.710 g, 13.60 mmol) in THF (40 ml) at 0°C. After the addition was complete, the mixture was allowed to warm at r.t. and further stirred for 22 h. The solvent was removed under vacuum and the resulting orange oil was dissolved in benzene (50 ml) and washed three times with water (200 ml). The organic layer was separated, dried over Na_2SO_4 and the benzene was evaporated under reduced pressure. The residue was dissolved in hexane (50 ml) again and filtered. Finally the filtrate was evaporated to dryness in vacuo and the 1.712 g of mixture of ruthenocene (10%), trimethylstannylruthenocene (**1**) (60%) and 1,1′-bis(trimethystannyl)ruthenocene (**2**) (30%) was obtained. This mixture was used for reaction without further purification.

1: Yellow oil. ^{1}H-NMR ($CDCl_3$): δ 4.69 (t, $J = 1.5$ Hz, 2H, C_5H_4), 4.50 (s, 5H, C_5H_5), 4.41 (t, $J = 1.5$ Hz, 2H, C_5H_4), 0.18 (s, $^2J_{Sn-H} = 53.2$, 56.1 Hz, 9H, Me). ^{13}C-NMR ($CDCl_3$): δ 111.0 (s, ipso C of C_5H_4), 75.68 (s, $J_{Pt-C} = 51.3$ Hz, C_5H_4), 72.26 (s, $J_{Pt-C} = 36.4$ Hz, C_5H_4), 69.94 (s, C_5H_5), −8.41 (s, $^1J_{Sn-C} = 361$, 346 Hz, Me).

2: Yellow oil. ^{1}H-NMR ($CDCl_3$): δ 4.62 (t, $J = 1.5$ Hz, 4H, C_5H_4), 4.39 (t, $J = 1.5$ Hz, 4H, C_5H_4), 0.18 (s, $^2J_{Sn-H} = 53.2$, 55.6 Hz, 18H, Me). ^{13}C-NMR ($CDCl_3$): δ 75.49 (s, $J_{Pt-C} = 51.3$ Hz, C_5H_4), 72.24 (s, $J_{Pt-C} = 36.4$ Hz, C_5H_4), −8.41 (s, $^1J_{Sn-C} = 361$, 344 Hz, Me). The resonance attributed to the C_5H_4 ipso carbons was not detected.

*3.2. Preparation of RcPt(cod)Cl (**3**) and {η^5-C_5H_4Pt-(cod)Cl}$_2$Ru (**4**)*

A 1.712 g of the mixture of ruthenocene (10%), trimethylstannylruthenocene (**1**) (60%) and 1,1′-bis(trimethystannyl)ruthenocene (**1**) (30%) was treated with Pt(cod)Cl_2 (1.614 g, 4.313 mmol) in THF (100 ml) under reflux for 4 h. The solvent was distilled off under reduced pressure and the residue was chromatographed over alumina. Elution with benzene gave the following bands in the order of elution: the pale yellow band of ruthenocene (145 mg, 85% recovery) and the yellow band of **3**. The solvent was removed from the second band in vacuo followed by recrystallization from CH_2Cl_2/hexane to give yellow crystals of **3** (955 mg) in 64% yield. CH_2Cl_2 fraction was concentrated to dryness and the residue was dissolved in CH_2Cl_2/benzene. Yellow precipitate of **4** (308 mg) was obtained in 37% yield by addition of hexane.

3: M.p. 163–167°C (dec.). ^{1}H-NMR ($CDCl_3$): δ 5.60 (t, $J = 2.6$ Hz, $^2J_{Pt-H} = 29.3$ Hz, 2H, =CH), 5.11 (t, $J = 2.6$ Hz, $^2J_{Pt-H} = 74.7$ Hz, 2H, =CH), 4.69 (t, $J = 1.8$ Hz, $J_{Pt-H} = 15.6$ Hz, 2H, C_5H_4), 4.60 (t, $J = 1.8$ Hz, 2H, C_5H_4), 4.59 (s, 5H, C_5H_5), 2.23–2.61 (m, 8H, CH_2). ^{13}C-NMR ($CDCl_3$): δ 112.0 (s, $^1J_{Pt-C} = 44.7$ Hz, =CH), 86.68 (s, $^1J_{Pt-C} = 205$ Hz, =CH), 80.94 (s, ipso C of C_5H_4), 73.58 (s, $J_{Pt-C} = 39.7$ Hz, C_5H_4), 71.23 (s, $J_{Pt-C} = 44.7$ Hz, C_5H_4), 70.16 (s, C_5H_5), 28.52 (s, CH_2). CV (in CH_2Cl_2, V vs. Ag/Ag$^+$): E_a 0.53, 0.80. Anal. Found; C, 38.12; H, 3.46; Cl, 6.50%. Calc. for $C_{18}H_{21}ClPtRu$: C, 38.00; H, 3.72; Cl, 6.23%.

4: M.p. 191–197°C (dec.). ^{1}H-NMR ($CDCl_3$): δ 5.58 (t, $J = 2.7$ Hz, $^2J_{Pt-H} = 24.4$ Hz, 4H, =CH), 5.17 (t, $J = 2.7$ Hz, $^2J_{Pt-H} = 76.1$ Hz, 4H, =CH), 4.76 (t, $J = 1.6$ Hz, 4H, C_5H_4), 4.62 (t, $J = 1.6$ Hz, 4H, C_5H_4), 2.25–2.65 (m, 16H, CH_2). ^{13}C-NMR ($CDCl_3$): δ 111.9 (s, $^1J_{Pt-C} = 44.7$ Hz, =CH), 86.69 (s, $^1J_{Pt-C} = 208$ Hz, =CH), 81.57 (s, ipso C of C_5H_4), 73.76 (s, $J_{Pt-C} = 38.1$ Hz, C_5H_4), 71.44 (s, $J_{Pt-C} = 39.7$ Hz, C_5H_4), 28.51 (s, CH_2). CV (in CH_2Cl_2, V vs. Ag/Ag$^+$): E_a 0.35, 0.58. Anal. Found; C, 34.25; H, 3.33; Cl, 7.77%. Calc. for $C_{26}H_{32}Cl_2Pt_2Ru$: C, 34.44; H, 3.56; Cl, 7.82%.

*3.3. Preparation of trans-RcPt(PEt$_3$)$_2$Cl (**5a**)*

To a solution of RcPt(cod)Cl (**3**) (102 mg, 0.179 mmol) in CH_2Cl_2 (30 ml) was added a 1.0 M solution of PEt_3 in THF (0.36 ml, 0.36 mmol) and the mixture was stirred for 2 h at r.t. After removal of the solvent in vacuo, the residue recrystallized from hexane gave pale yellow crystals (106 mg, yield 85%). M.p. 107–108°C. ^{1}H-NMR($CDCl_3$): δ 4.46 (t, $J = 1.5$ Hz, 2H, C_5H_4), 4.34 (s, 5H, C_5H_5), 4.27 (t, $J = 1.5$ Hz, $J_{Pt-H} = 28.3$ Hz, 2H, C_5H_4), 1.97–1.89 (m, 12H, CH_2), 1.10 (quintet, $J = 7.8$ Hz, 18H, CH_3). ^{13}C-NMR ($CDCl_3$): δ 85.74 (t, $^2J_{P-C} = 8.3$ Hz, ipso C of C_5H_4), 78.07 (s, $J_{Pt-C} = 72.8$ Hz, C_5H_4), 71.09 (s, C_5H_5), 67.75 (s, $J_{Pt-C} = 61.2$ Hz, C_5H_4), 12.40 (t, $J = 16.5$ Hz, CH_2), 7.93 (s, CH_3). ^{31}P-NMR ($CDCl_3$): δ 22.15 (s, $^1J_{Pt-P} = 2714$ Hz). Anal. Found: C, 38.03; H, 5.48; Cl, 5.00; P, 8.73%. Calc. for $C_{22}H_{39}ClP_2PtRu$: C, 37.91; H, 5.64; Cl, 5.09; P, 8.89%.

*3.4. Preparation of trans-RcPt(PEt$_3$)$_2$Br (**5b**)*

To a solution of **5a** (470 mg, 0.674 mmol) in methanol (20 ml) was added a solution of NaBr (560 mg, 5.44 mmol) in 30 ml of methanol and stirred for 3 h at r.t. After removal of the solvent in vacuo, the residue was dissolved in 50 ml of benzene and washed with 250 ml of water for three times. Organic layer was dried over Na_2SO_4 and benzene was evaporated under vacuum again. Recrystallization from hexane gave pale yellow crystals (437 mg, yield 87%). M.p. 135–136°C. ^{1}H-NMR ($CDCl_3$): δ 4.48 (t, $J = 1.5$ Hz, 2H, C_5H_4), 4.35 (s, 5H, C_5H_5), 4.28 (t, $J = 1.5$ Hz, $J_{Pt-H} = 29.3$ Hz, 2H, C_5H_4), 2.03–1.96 (m, 12H, CH_2), 1.09 (quintet, $J = 7.9$ Hz, 18H, CH_3). ^{13}C-NMR ($CDCl_3$): δ 88.78 (t, $^2J_{P-C} = 8.3$ Hz, ipso C of C_5H_4), 77.92 (s, $J_{Pt-C} = 74.4$ Hz, C_5H_4), 71.22 (s, C_5H_5), 67.72 (s, $J_{Pt-C} = 62.9$ Hz, C_5H_4), 13.14 (t, $J = 16.5$ Hz, CH_2), 8.01 (s, CH_3). ^{31}P-NMR ($CDCl_3$): δ 19.81 (s, $^1J_{Pt-P} = 2693$ Hz). Anal. Found: C, 35.84; H, 5.26; Br, 10.66; P, 8.45%. Calc. for $C_{22}H_{39}BrP_2PtRu$: C, 35.65; H, 5.30; Br, 10.78; P, 8.35%.

3.5. Preparation of *trans*-$RcPt(PEt_3)_2NCS$ (**5c**)

As described in the preparation of **5b**, treatment of **5a** (397 mg, 0.569 mmol) with NaSCN (389 mg, 4.79 mmol) in 50 ml of acetone gave pale yellow crystals (387 mg, yield 95%). M.p. 117–118°C. IR (KBr): ν(NCS) 2100 cm^{-1}. ^{1}H-NMR ($CDCl_3$): δ 4.47 (t, $J =$ 1.2 Hz, 2H, C_5H_4), 4.33 (s, 5H, C_5H_5), 4.17 (t, $J = 1.2$ Hz, $J_{Pt-H} = 25.4$ Hz, 2H, C_5H_4), 1.91–1.84 (m, 12H, CH_2), 1.12 (quintet, $J = 7.9$ Hz, 18H, CH_3). ^{13}C-NMR ($CDCl_3$): δ 134.0 (s, NCS), 80.58 (s, ipso C of C_5H_4), 77.89 (s, $J_{Pt-C} = 64.5$ Hz, C_5H_4), 71.03 (s, C_5H_5), 68.17 (s, $J_{Pt-C} = 54.6$ Hz, C_5H_4), 13.02 (t, $J = 16.5$ Hz, CH_2), 7.88 (s, CH_3). ^{31}P-NMR ($CDCl_3$): δ 23.88 (s, $^1J_{Pt-P} =$ 2654 Hz). Anal. Found: C, 38.24; H, 5.46; N, 1.94; P, 8.67%. Calc. for $C_{23}H_{39}NP_2PtRuS$: C, 38.36; H, 5.46; N, 1.95; P, 8.61%.

3.6. Reaction of *trans*-$RcPt(PEt_3)_2Cl$ (**5a**) with CO

A dichloromethane solution of **5a** (50 mg, 0.072 mmol) was placed in 100 ml of autoclave and charged with CO (30 kg cm^{-2}). After standing for 24 h at r.t., the solvent was removed under vacuum. Pale yellow crystals of **7a** (46 mg, yield 88%) were obtained by recrystallization of toluene/hexane. M.p. 153–154°C. IR (KBr): ν(C=O) 1610 cm^{-1}. ^{1}H-NMR ($CDCl_3$): δ 5.09 (s, 2H, C_5H_4), 4.58 (s, 2H, C_5H_4), 4.52 (s, 5H, C_5H_5), 1.93–1.75 (m, 12H, CH_2), 1.15 (quintet, $J = 7.9$ Hz, 18H, CH_3). ^{13}C-NMR ($CDCl_3$): δ 211.6 (s, CO), 101.1 (t, $^3J_{P-C} = 4.1$ Hz, ipso C of C_5H_4), 71.45 (s, C_5H_5), 71.16 (s, C_5H_4), 70.42 (s, C_5H_4), 14.18 (t, $J =$ 16.5 Hz, CH_2), 7.81 (s, CH_3). ^{31}P-NMR ($CDCl_3$): δ 16.61 (s, $^1J_{Pt-P} = 3044$ Hz). Anal. Found: C, 38.01; H, 5.34; Cl, 4.74; P, 8.32%. Calc. for $C_{23}H_{39}ClOP_2PtRu$: C, 38.10; H, 5.42; Cl, 4.89; P, 8.54%.

3.7. Reaction of *trans*-$RcPt(PEt_3)_2Br$ (**5b**) with CO

This reaction was carried out by a procedure similar to that of **5a**.

7b: Pale yellow crystals, yield 88%, m.p. 160–161°C. IR (KBr): ν(C=O) 1590 cm^{-1}. ^{1}H-NMR ($CDCl_3$): δ 5.09 (s, 2H, C_5H_4), 4.57 (s, 2H, C_5H_4), 4.52 (s, 5H, C_5H_5), 1.99–1.80 (m, 12H, CH_2), 1.14 (quintet, $J = 7.9$ Hz, 18H, CH_3). ^{13}C-NMR ($CDCl_3$): δ 212.2 (t, $^2J_{P-C} =$ 5.8 Hz, CO), 100.7 (t, $^2J_{Pt-C} = 261$ Hz, $^3J_{P-C} = 5.0$ Hz, ipso C of C_5H_4), 71.50 (s, C_5H_5), 71.26 (s, C_5H_4), 70.45 (s, C_5H_4), 14.72 (t, $J = 16.5$ Hz, CH_2), 7.89 (s, CH_3). ^{31}P-NMR ($CDCl_3$): δ 16.46 (s, $^1J_{Pt-P} = 3031$ Hz). Anal. Found: C, 36.01; H, 5.15; Br, 10.44; P, 8.05%. Calc. for $C_{23}H_{39}BrOP_2PtRu$: C, 35.90; H, 5.11; Br, 10.38; P, 8.05%.

3.8. Reaction of *trans*-$RcPt(PEt_3)_2Cl$ (**5a**) with *p*-tolyl isocyanide

To a 20 ml of 1,2-dichloroethane of complex **5a** (152 mg, 0.218 mmol) was added *p*-tolyl isocyanide (31 mg, 0.26 mmol). The reaction mixture was stirred for 6 h at reflux temperature. After removal of the solvent under vacuum, the residue was chromatographed on alumina using chloroform as an eluent. Yellow crystals of **9a** (111 mg, yield 63%) was obtained by recrystallization from toluene/hexane. M.p. 182–183°C. IR (KBr): ν(C=N) 1550 cm^{-1}. ^{1}H-NMR ($CDCl_3$): δ 7.60 (d, $J = 8.3$ Hz, 2H, Ar), 7.06 (d, $J = 8.3$ Hz, 2H, Ar), 5.19 (s, 2H, C_5H_4), 4.56 (s, 5H, C_5H_5), 4.55 (s, 2H, C_5H_4), 2.28 (s, 3H, $ArCH_3$), 1.83–1.60 (m, 12H, CH_2), 1.03 (quintet, $J = 7.8$ Hz, 18H, PCH_2CH_3). ^{13}C-NMR ($CDCl_3$): δ 172.1 (t, $^2J_{P-C} = 7.4$ Hz, C=N), 151.2 (s, $^2J_{Pt-C} = 72.8$ Hz, ipso C of Ar bound to –N=C), 133.1 (s, ipso C of Ar bound to CH_3), 128.5 (s, Ar), 121.1 (s, Ar), 101.6 (s, ipso C of C_5H_4), 73.31 (s, C_5H_4), 71.37 (s, C_5H_5), 69.60 (s, C_5H_4), 20.87 (s, $ArCH_3$), 14.93 (t, $J = 16.5$ Hz, CH_2), 8.01 (s, PCH_2CH_3). ^{31}P-NMR ($CDCl_3$): δ 14.70 (s, $^1J_{Pt-P} = 2894$ Hz). Anal. Found: C, 44.20; H, 5.72; N, 1.71; Cl, 4.22; P, 7.57%. Calc. for $C_{30}H_{46}NClP_2PtRu$: C, 44.25; H, 5.69; N, 1.72; Cl, 4.35; P, 7.61%.

3.9. Reaction of *trans*-$RcPt(PEt_3)_2Cl$ (**5a**) with 2,6-xylyl or *p*-nitrophenyl isocyanide

These reactions were performed by a procedure similar to that with *p*-tolyl isocyanide.

9b: Yellow crystals, yield 36%, m.p. 198–199°C. IR (KBr): ν(C=N) 1555 cm^{-1}. ^{1}H-NMR ($CDCl_3$): δ 6.94 (d, $J = 7.3$ Hz, 2H, Ar), 6.82 (t, $J = 7.3$ Hz, 1H, Ar), 5.29 (s, 2H, C_5H_4), 4.55 (s, 2H, C_5H_4), 4.54 (s, 5H, C_5H_5), 2.49 (s, 6H, $ArCH_3$), 1.75–1.63 (m, 12H, CH_2), 1.03 (quintet, $J = 7.8$ Hz, 18H, PCH_2CH_3). ^{13}C-NMR ($CDCl_3$): δ 168.0 (s, C=N), 149.7 (s, ipso C of Ar bound to –N=C), 128.5 (s, Ar), 128.3 (s, ipso C of Ar bound to CH_3), 122.4 (s, Ar), 104.5 (s, ipso C of C_5H_4), 73.25 (s, C_5H_4), 71.12 (s, C_5H_5), 69.01 (s, C_5H_4), 21.49 (s, $ArCH_3$), 15.40 (t, $J = 16.5$ Hz, CH_2), 8.36 (s, PCH_2CH_3). ^{31}P-NMR ($CDCl_3$): δ 13.92 (s, $^1J_{Pt-P} =$ 2992 Hz). Anal. Found: C, 45.00; H, 5.58; N, 1.76; Cl, 4.56; P, 7.30%. Calc. for $C_{31}H_{48}NClP_2PtRu$: C, 44.95; H, 5.84; N, 1.69; Cl, 4.28; P, 7.48%.

9c: Yellow orange crystals, yield 50%, m.p. 196–197°C. IR (KBr): ν(C=N) 1535 cm^{-1}. ^{1}H-NMR ($CDCl_3$): δ 8.16 (d, $J = 8.8$ Hz, 2H, Ar), 7.70 (d, $J = 8.8$ Hz, 2H, Ar), 5.21 (s, 2H, C_5H_4), 4.61 (s, 2H, C_5H_4), 4.56 (s, 5H, C_5H_5), 1.86–1.65 (m, 12H, CH_2), 1.03 (quintet, $J = 7.9$ Hz, 18H, CH_3). ^{13}C-NMR ($CDCl_3$): δ 181.0 (t, $^{2}J_{P-C} = 6.6$ Hz, C=N), 159.4 (s, $^{3}J_{Pt-C} = 71.1$ Hz, ipso C of Ar bound to –N=C), 143.2 (s, ipso C of Ar bound to NO_2), 124.1 (s, Ar), 121.0 (s, Ar), 101.0 (s, ipso C of C_5H_4), 73.44 (s, C_5H_4), 71.63 (s, C_5H_5), 70.31 (s, C_5H_4), 14.97 (t, $J = 16.5$ Hz, CH_2), 8.05 (s, CH_3). ^{31}P-NMR ($CDCl_3$): δ 15.52 (s, $^{1}J_{Pt-P} = 2809$ Hz). Anal. Found: C, 41.20; H, 5.18; N, 3.32; Cl, 4.19; P, 7.29%. Calc. for $C_{29}H_{43}N_2ClO_2P_2PtRu$: C, 41.21; H, 5.13; N, 3.31; Cl, 4.19; P, 7.33%.

*3.10. Reaction of trans-RcPt(PEt$_3$)$_2$Cl (**5a**) with dimethyl acetylenedicarboxylate (DMAD)*

To a solution of **5a** (126 mg, 0.180 mmol) in benzene (20 ml) was added DMAD (26 mg, 0.18 mmol) and the mixture was stirred at 80°C for 24 h. After removal of the solvent in vacuo, the residue purified by chromatography on alumina using CH_2Cl_2 as an eluent. Recrystallization from toluene/hexane gave yellow crystals of **11a** (37 mg) in 25% yield. M.p. 166–167°C. IR (KBr): ν(C=O) 1735, 1705, ν(C=C) 1610 cm^{-1}. ^{1}H-NMR ($CDCl_3$): δ 7.94 (s, 1H, =CH), 4.67 (t, $J = 2.4$ Hz, 1H, C_5H_3), 4.63 (dd, $J = 1.0$, 1.5 Hz, 1H, C_5H_3), 4.52 (s, $J_{Pt-H} = 32.7$ Hz, 1H, C_5H_3), 4.37 (s, 5H, C_5H_5), 3.88 (s, 3H, OCH_3), 3.66 (s, 3H, OCH_3), 2.48–1.95 (m, 6H, CH_2), 1.61–1.56 (m, 6H, CH_2), 1.22–1.14 (m, 9H, PCH_2CH_3), 1.04–0.96 (m, 9H, PCH_2CH_3). ^{13}C-NMR ($CDCl_3$): δ 169.5 (s, CO), 166.5 (s, CO), 153.0 (s, =C), 110.7 (s, =CH), 87.07 (t, $^{2}J_{P-C} = 8.3$ Hz, ipso C of C_5H_3 bound to Pt), 84.01 (s, $^{2}J_{Pt-C} = 41.4$ Hz, ipso C of C_5H_3 bound to –C=C), 81.34 (s, $J_{Pt-C} = 56.2$ Hz, C_5H_3), 73.03 (s, C_5H_5), 71.01 (s, $J_{Pt-C} = 67.8$ Hz, C_5H_3), 69.89 (s, $J_{Pt-C} = 44.7$ Hz, C_5H_3), 52.24 (s, OCH_3), 51.35 (s, OCH_3), 13.31 (dd, $^{1}J_{P-C} = 21.5$ Hz, $^{3}J_{P-C} = 11.6$ Hz, CH_2), 11.38 (dd, $^{1}J_{P-C} = 23.2$ Hz, $^{3}J_{P-C} = 9.9$ Hz, CH_2), 7.76 (s, PCH_2CH_3), 7.66 (s, PCH_2CH_3). ^{31}P-NMR ($CDCl_3$): δ 18.75 (d, $^{1}J_{Pt-P} = 2605$ Hz, $^{2}J_{P-P} = 417$ Hz), 17.68 (d, $^{1}J_{Pt-P} = 2686$ Hz, $^{2}J_{P-P} = 417$ Hz). Anal. Found: C, 40.22; H, 5.40; Cl, 4.50; P, 7.11%. Calc. for $C_{28}H_{45}ClO_4P_2PtRu$: C, 40.07; H, 5.40; Cl, 4.22; P, 7.38%.

*3.11. Reaction of trans-RcPt(PEt$_3$)$_2$Br (**5b**) with DMAD*

This reaction was performed by a procedure similar to that of **5a**.

11b: Yellow crystals, yield 40%, m.p. 154–155°C. IR (KBr): ν(C=O) 1730, 1705, ν (C=C) 1610 cm^{-1}. ^{1}H-NMR ($CDCl_3$): δ 7.88 (s, 1H, =CH), 4.69 (t, $J = 2.0$ Hz, 1H, C_5H_3), 4.65 (s, 1H, C_5H_3), 4.52 (s, $J_{Pt-H} = 32.2$ Hz, 1H, C_5H_3), 4.37 (s, 5H, C_5H_5), 3.88 (s, 3H, OCH_3), 3.66 (s, 3H, OCH_3), 2.56–1.98 (m, 6H, CH_2), 1.69–1.63 (m, 6H, CH_2), 1.21–1.13 (m, 9H, PCH_2CH_3), 1.03–0.95 (m, 9H, PCH_2CH_3). ^{13}C-NMR ($CDCl_3$): δ 169.5 (s, CO), 166.5 (s, CO), 152.9 (s, =C), 110.6 (s, =CH), 89.96 (t, $^{2}J_{P-C} = 8.3$ Hz, ipso C of C_5H_3 bound to Pt), 84.16 (s, $^{2}J_{Pt-C} = 43.0$ Hz, ipso C of C_5H_3 bound to –C=C), 81.22 (s, $J_{Pt-C} = 61.2$ Hz, C_5H_3), 73.22 (s, C_5H_5), 70.98 (s, $J_{Pt-C} = 66.2$ Hz, C_5H_3), 69.98 (s, $J_{Pt-C} = 46.3$ Hz, C_5H_3), 52.29 (s, OCH_3), 51.42 (s, OCH_3), 13.90 (dd, $^{1}J_{P-C} = 21.5$ Hz, $^{3}J_{P-C} = 9.9$ Hz, CH_2), 12.30 (dd, $^{1}J_{P-C} = 24.8$ Hz, $^{3}J_{P-C} = 9.9$ Hz, CH_2), 7.88 (s, PCH_2CH_3). ^{31}P-NMR ($CDCl_3$): δ 18.05 (d, $^{1}J_{Pt-P} = 2586$ Hz, $^{2}J_{P-P} = 414$ Hz), 16.82 (d, $^{1}J_{Pt-P} = 2652$ Hz, $^{2}J_{P-P} = 414$ Hz). Anal. Found: C, 38.15; H, 5.14; Br, 9.01; P, 6.93%. Calc. for $C_{28}H_{45}BrO_4P_2PtRu$: C, 38.06; H, 5.13; Br, 9.04; P, 7.01%.

*3.12. Reaction of trans-RcPt(PEt$_3$)$_2$Cl (**5a**) with diethyl acetylenedicarboxylate*

This reaction was also carried out by a procedure similar to that with DMAD.

11c: Yellow crystals, yield 30%, m.p. 127–128°C. IR (KBr): ν(C=O) 1730, 1705, ν (C=C) 1610 cm^{-1}. ^{1}H-NMR ($CDCl_3$): δ 7.89 (s, 1H, =CH), 4.66 (s, 1H, C_5H_3), 4.65 (s, 1H, C_5H_3), 4.52 (s, 1H, C_5H_3), 4.37 (s, 5H, C_5H_5), 4.34 (quartet, $J = 7.1$ Hz, 2H, OCH_2), 4.12 (d quartet, $J = 7.3$, 2.0 Hz, 2H, OCH_2), 2.50–1.94 (m, 6H, PCH_2), 1.59 (quartet, $J = 7.2$ Hz, 6H, PCH_2), 1.39 (t, $J = 7.1$ Hz, 3H, OCH_2CH_3), 1.21 (t, $J = 7.1$ Hz, OCH_2CH_3), 1.23–1.12 (m, 9H, PCH_2CH_3), 1.04–0.96 (m, 9H, PCH_2CH_3). ^{13}C-NMR ($CDCl_3$): δ 169.0 (s, CO), 165.9 (s, CO), 152.7 (s, =C), 111.2 (s, =CH), 86.82 (t, $^{2}J_{P-C} = 8.3$ Hz, ipso C of C_5H_3 bound to Pt), 84.19 (s, $^{2}J_{Pt-C} = 41.4$ Hz, ipso C of C_5H_3 bound to –C=C), 81.16 (s, $J_{Pt-C} = 61.2$ Hz, C_5H_3), 72.92 (s, C_5H_5), 70.86 (s, $J_{Pt-C} = 67.8$ Hz, C_5H_3), 69.68 (s, $J_{Pt-C} = 44.7$ Hz, C_5H_3), 61.06 (s, OCH_2), 59.82 (s, OCH_2), 14.18 (s, OCH_2CH_3), 14.05 (s, OCH_2CH_3), 13.22 (dd, $^{1}J_{P-C} = 21.5$ Hz, $^{3}J_{P-C} = 9.9$ Hz, PCH_2), 11.31 (dd, $^{1}J_{P-C} = 24.8$ Hz, $^{3}J_{P-C} = 9.9$ Hz, PCH_2), 7.73 (s, PCH_2CH_3), 7.60 (s, PCH_2CH_3). ^{31}P-NMR ($CDCl_3$): δ 18.34 (d, $^{1}J_{Pt-P} = 2611$ Hz, $^{2}J_{P-P} = 417$ Hz), 16.95 (d, $^{1}J_{Pt-P} = 2686$ Hz, $^{2}J_{P-P} = 417$ Hz). Anal. Found: C, 41.79; H, 5.72; Cl, 4.25; P, 7.00%. Calc. for $C_{30}H_{49}ClO_4P_2PtRu$: C, 41.55; H, 5.69; Cl, 4.09; P, 7.14%.

3.13. X-ray crystallographic studies

Single crystals of **3**, **4**, **5c** and **9a** suitable for an X-ray diffraction analysis were obtained by cooling of

CH_2Cl_2/hexane solution of **3** at -10°C, slow evaporation of CH_2Cl_2 solution of **4** at r.t., slow evaporation of hexane solution for **5c** at r.t. and cooling of toluene/hexane solution at -10°C for **9a**, respectively, and mounted on glass fibers with epoxy resin. Diffraction measurements were made on a Rigaku AFC5R diffractometer with graphite monochromated Mo–K_α radiation ($\lambda = 0.71069$ Å) using $\omega/2\theta$ scan technique with a scan rate 8° min^{-1} for **3** and **4** or 16° min^{-1} for **5c** and **9a**. Unit cells were determined and refined by a least-square method using 25 reflections in the range $34 < 2\theta < 35°$ for **3**, **4** and **5c**, and 25 reflections in the range $24 < 2\theta < 30°$ for **9a**. The data of weak reflections ($I < 10\sigma(I)$) were measured twice and averaged. Three standard reflections were monitored at every 150 measurements and no damage was observed. Intensities were collected for Lorentz and polarization effects and an empirical absorption collection was made using ψ-scan technique. Relevant crystal data are given in Table 5.

The positions of metal atoms were located by Patterson method. Subsequent difference Fourier maps revealed the positions of all non-hydrogen atoms. All non-hydrogen atoms were refined anisotropically and all hydrogen atoms were included at the calculated positions using isotropic thermal parameters. The final cycles of full-matrix least-squares refinement were converged, and the largest parameter shifts against errors were 0.01 for **3**, 0.36 for **4**, 0.63 for **5c**, and 0.86 for **7a**, respectively. The unweighted and weighted agreement factors are $R = \Sigma\|F_o| - |F_c\|/\Sigma|F_o| = 0.026$ and $R_w = [\Sigma w(|F_o| - |F_c|)^2/\Sigma wF_o^2]^{0.5} = 0.029$ for **3**, $R = 0.032$ and $R_w = 0.036$ for **4**, $R = 0.036$ and $R_w = 0.035$ for **5c**, and $R = 0.064$ and $R_w = 0.056$ for **7a**, respectively. All calculation were performed on VAX station 3100 using the teXsan crystallographic software package.

Acknowledgements

This work is supported by Grant-in-Aid for Scientific Research from The Ministry of Education, Science, Sports and Culture.

References

[1] A. Togni, T. Hayashi (Eds.), Ferrocenes, VCH, Weinheim, 1995.

[2] M. Rosenblum, Chemisty of the Iron Group Metallocenes, Wiley, New York, 1965.

[3] (a) G.L. Hardgrove, D.H. Templeton, Acta Crystallogr. 12 (1959) 28. (b) J.D. Dunitz, L.E. Orgel, A. Rich, Acta Crystallogr. 9 (1956) 373.

[4] S.P. Gubin, S.A. Smirnova, L.I. Penisovich, A.A. Lubovich, J. Organomet. Chem. 30 (1971) 243.

[5] (a) V.G. Andrianov, Y.T. Struchkov, E.R. Rossinskaya, J. Chem. Soc. Chem. Commun. (1973) 338. (b) A.N. Nesmeyanov, Y.T. Struchkov, N.N. Sedova, V.G. Andrianov, Y.V. Volgin, V.A. Sazonova, J. Organomet. Chem. 137 (1977) 217. (c) A.N. Nesmeyanov, N.N. Sedova, Y.T. Struchkov, V.G. Andrianov, E.N. Stakheeva, V.A. Sazonova, J. Organomet. Chem. 153 (1978) 115. (d) D. Seyferth, B.W. Hames, T.G. Rucker, M. Cowie, R.S. Dickson, Organometallics 2 (1983) 472. (e) M. Cowie, R.S. Dickson, J. Organomet. Chem. 326 (1987) 269. (f) S. Akabori, T. Kumagai, T. Shirahige, S. Sato, K. Kawazoe, C. Tamura, Organometallics 6 (1987) 2105. (g) M.I. Bruce, P.A. Humphrey, O. bin Shawkataly, M.R. Snow, E.R.T. Tiekink, W.R. Cullen, Organometallics 9 (1990) 2910. (h) W.R. Cullen, S.J. Rettig, T.-C. Zheng, Organometallics 11 (1992) 277. (i) M. Sato, K. Suzuki, H, Asano, M. Sekino, Y. Kawata. Y. Habata, S. Akabori, J. Organomet. Chem. 473 (1994) 263.

[6] T. Yoshida, S. Tanaka, T. Adachi, T. Yoshida, K. Onitsuka, K. Sonogashira, Angew. Chem. Int. Ed. Engl. 34 (1995) 319.

[7] T. Yoshida, K. Onitsuka, K. Sonogashira, J. Organomet. Chem. 511 (1996) 47.

[8] K. Onitsuka, T. Yoshida, T. Adachi, T. Yoshida, K. Sonogashira, Chem. Lett. (1995) 233.

[9] (a) H. Bürger, C. Kluess, Z. Anorg. Allg. Chem. 423 (1976) 112. (b) S. Kamiyama, T. Kimura, A. Kasahara, T. Izumi, M. Maemura, Bull. Chem. Soc. Jpn. 52 (1979) 142.

[10] Z. Dawoodi, C. Eaborn, A. Pidcock, J. Organomet. Chem. 170 (1979) 95.

[11] T. Yoshida, S. Tanaka, K. Shiina, K. Sonogashira, unpublished results.

[12] E.O. Fischer, M. von Foerster, C.G. Kreiter, K.E. Schwarzhans, J. Organomet. Chem. 7 (1967) 113.

[13] N. Fujita, K. Sonogashira, J. Polym. Sci. Polym. Chem. Ed. 12 (1973) 1471.

[14] R.E. Hollands, A.G. Osborne, R.H. Whiteley, C.J. Cardin, J. Chem. Soc. Dalton Trans. (1985) 1527.

[15] K. Onitsuka, N. Hosokawa, T. Adachi, T. Yoshida, K. Sonogashira, Chem. Lett. (1994) 1985.

[16] G. Booth, J. Chatt, J. Chem. Soc. A (1966) 634.

[17] (a) K.P. Wagner, P.M. Treichel, J.C. Calagrese, J. Organomet. Chem. 71 (1974) 299. (b) K. Onitsuka, K. Murakami, K. Matsukawa, K. Sonogashira, T. Adachi, T. Yoshida, J. Organomet. Chem. 490 (1995) 117.

[18] G.K. Anderson, R.J. Cross, Acc. Chem. Res. 17 (1984) 67.

[19] W.P. Weber, G.W. Gokel, Tetrahedron Lett. 17 (1972) 1637.